CIVIL ENGINEERING JOURNAL

Article no. 28

THE CIVIL ENGINEERING JOURNAL 2-2021

STUDY ON ADJUSTABLE CONNECTOR OF RECIPROCAL FRAME

Lin Qi, Zifei Li, Lingtong Li, Hui Pan, Zhenzhou Xie and Xin Huang

Civil Aviation University of China, Tianjin, China; qilin1208@vip.163.com

ABSTRACT

In this paper, we design an adjustable connector of reciprocal frame, and a three-dimensional solid model of this connector with Circular Hollow Section has been created in the FEM software Abaqus CAE to study its mechanical properties. When the plastic hinge is formed at the end of the Circular Hollow Section, the connector is still in an elastic state. It is concluded that the adjustable connector of reciprocal frame has high strength and rigidity, realizing the goal for designing higher connector strength over Circular Hollow Section strength. Then parametric analysis is used to analyse the influence of the connector about each part on the mechanical properties, and the flexural rigidity of the connector has been derived. A three-dimensional wire model of reciprocal frames has been created in the FEM software Abaqus CAE, and a full-scale test model of the structure is designed. The numerical simulation results agree well with the test results. It is verified that the reliability of the modeling method and the accuracy of the connector mechanical model.

KEYWORD

Reciprocal frame, Connector of reciprocal frame, Numerical model of connector, Mechanical model of connector, Full-scale test

INTRODUCTION

Reciprocal frame is a special structure [1]. In reciprocal frames, members are mutually supported, to be more specific, a member supports an adjacent counterpart and is supported by another in return [2-4]. Figure1 indicates a common circular reciprocal frame [4]. Thanks to its unique and mutually supported feature, the members and connectors of reciprocal frame are in a simple and unified structure [5]. Therefore, reciprocal frame can simplify the on-site assembling process and draws an extensive attention in the field of prefabricated building [6-8].

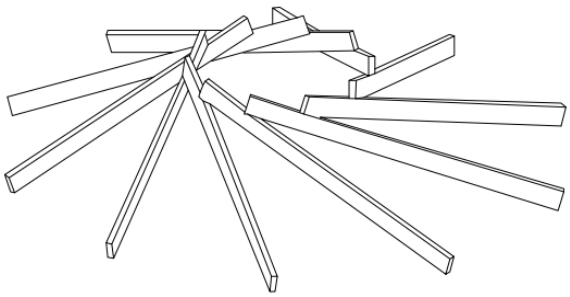

Fig. 1 - A circular reciprocal frame

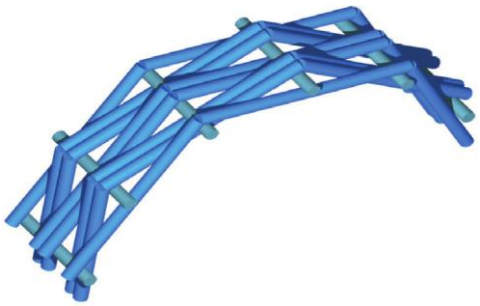

Fig.2 - Model of Chinese laminated beam bridge

Due to the unique construction nature of reciprocal frame, the function of connector is attached with great importance. The stability and reliability of a reciprocal frame directly influence its

performance. Reciprocal frame has various types of joints. Figure 2 is a model of laminated beam bridge in ancient China [9], and Figure 3 shows an example of woven closed geodesic basket [10]. The joints of the two reciprocal frame models mentioned above are inter-locked, depending on the frictional force to ensure the strong connection of whole frame. The connection process of this friction-driven joints is simple, but the strength and rigidity of the joints are weak which proposes limitation on the size of reciprocal frame [11-13]. New methods of connection such as lashed connection (Figure 4.) and notched connection (Figure 5.) have appeared with the advancement of reciprocal frame. However, because of the weak strength and rigidity of these two methods, the strength and rigidity of reciprocal frame are greatly reduced at the same time [14-15] New methods of connection such as lashed connection (Figure 4.) and notched connection (Figure 5.) have appeared with the advancement of reciprocal frame. However, because of the weak strength and rigidity of these two methods, the strength and rigidity of reciprocal frame are greatly reduced at the same time [14-15].

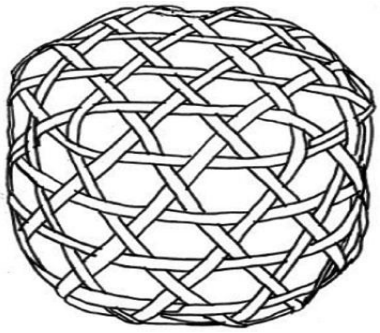

Fig.3 - Woven closed basket

Fig. 4 - Lashed connections

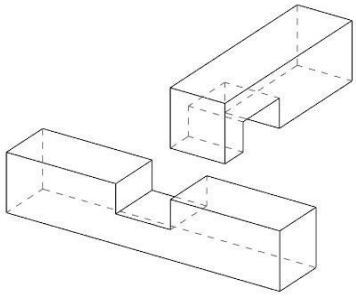

Fig. 5 - Notched connection

In 1976, Bijnen published the first patent concerning with reciprocal frame's connector Bolted Connectors [16]. He suggested to loop steel pipes via threaded pins to form a closed-circuit structure. As can be seen from Figure 6, the joint is achieved in a simple way, and the strength and rigidity are high. On the contrary, this connector requires high accuracy in terms of connecting threaded pins and reserved holes. As a result, it presents difficulties for on-site construction and reduces construction efficiency. Moreover, two members connected by one threaded pin can rotate around the pin, affecting the rigidity of the entire structure [17-18]. In recent years, temporary reciprocal-frame buildings have received wide attention, and the application of scaffolding swivel couplers can be observed in reciprocal frame (Figure 7). Scaffolding swivel coupler has great tolerance for error, but this connector is of little strength and rigidity. It is mostly used for temporary buildings as it is difficult to ensure the stability, rigidity and seismic performance of the structure [19-20] Figure 8 is an example of coupler connector [14]. Coupler connector owns the features of large strength and rigidity and high construction accuracy. What is more, it can only be applied to vertically connected members, and the application scope of its connector is limited as well [15].

Fig. 6 - Bolted connectors

Fig. 7 - Scaffolding swivel couplers

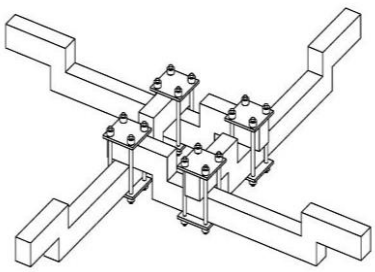

Fig.8 - Coupler connectors

In conclusion, though there are various types of connections of reciprocal frame, most of them face the issues of poor strength and rigidity or limited application scope. Consequently, it is crucial to conduct studies on exploring new types of reciprocal frame connector of better strength and rigidity and wider application scope.

ADJUSTABLE CONNECTOR OF RECIPROCAL FRAME

In order to overcome the connector of reciprocal frame's existing problems of low strength and rigidity and small range of application, this paper designs an adjustable connector of reciprocal frame with higher strength and rigidity, and this connector can compensate for the installation error of the reciprocal frame members. As shown in Figure 9, the connector consists of upper and lower semi-connectors, each of which is composed of a sleeve (1), a nut (2) and a connecting plate (3) with four arc-shaped holes.

The inner diameter of the sleeve fits with the outer diameter of the Circular Hollow Section. Besides, a certain length of thread is machined on the outer walls of both ends of the Circular Hollow Section for adjusting the relative position between Circular Hollow Section and sleeve when there are errors in the freedom of the point during installation and therefore the member bar and sleeve can be tightened by nut.

The connecting plates of the upper and lower hemi-connectors are connected by bolts that pass through the arc-shaped holes on the connecting plate. Since the arc-shaped connecting hole is larger than the diameter of the bolt rod, the upper and lower connecting plates can rotate relatively to each other in order to eliminate the error during installation. After properly adjusting the relative rotation angle of the connecting plate between upper and lower hemi-connectors, arc-shaped holes will be filled with FastSteel.

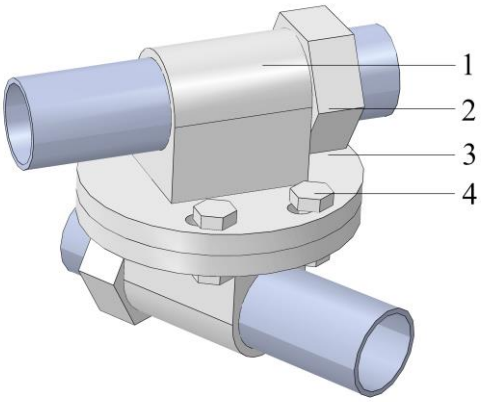

Fig. 9 - The model adjustable connector of reciprocal frame

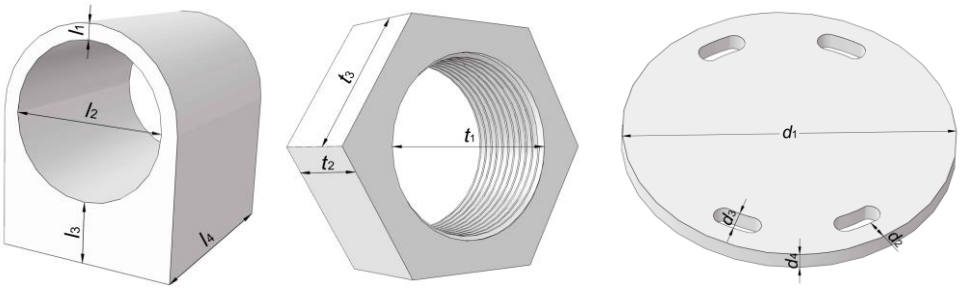

（1）Sleeve　　（2）Nut　　（3）Connecting plate

Fig.10 - The geometric parameters of the parts in the connector of reciprocal frame

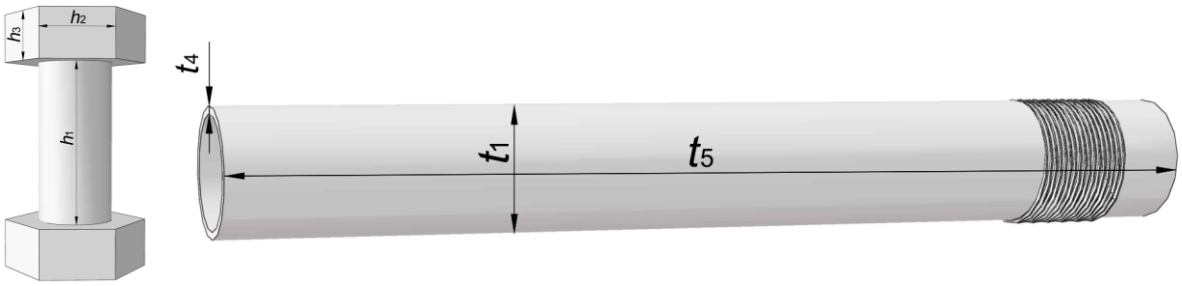

（4）Bolt （5）Circular Hollow Section

Fig.10 - The geometric parameters of the parts in the connector of reciprocal frame

NUMERICAL ANALYSIS OF ADJUSTABLE CONNECTOR OF RECIPROCAL FRAME

Mechanical characteristics of connector

A three-dimensional solid model of the connector has been created in the FEM software Abaqus CAE to study the mechanical properties of the connector. The parameters of each part of the connector are shown in Table 1.

Tab.1 - The geometric parameters of the connector/mm

Geometric Parameters	d_1	d_2	d_3	d_4	l_1	l_2	l_3	l_4	t_1	t_2	t_3	t_4	t_5	h_1	h_2	h_3
Value	180	16	16	15	6	60	30	90	60	46	30	6	490	30	12	10

This connector is made of Q235 steel and it applies with Class 10.9 M16 bolts. The upper and lower connector plates, the sleeve and the Circular Hollow Sections, and the bolt and the connector plate are connected in a hard contact way.

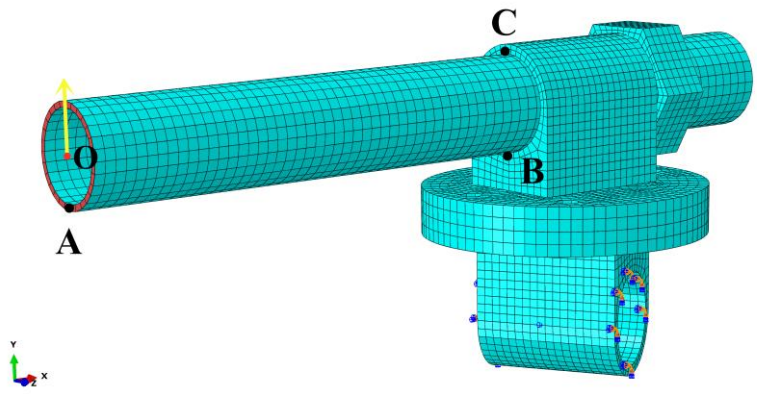

Fig. 11 - Finite element numerical model under Y-direction shearing force

The reciprocal frame members are mainly subjected to lateral loads which cause bending moments and shearing forces in the members. A shearing force parallel to the Y-axis is applied to the end section of the Circular Hollow Section as shown in Figure 11. In order to study the force characteristics and failure mechanism of this connector, the applied shearing force is continuously increased until the plastic deformation of the whole Circular Hollow Section has formed. Based on the analysis, the intersection of the Circular Hollow Section and the sleeve is the maximum force section of the Circular Hollow Section. When the shearing force parallel to the Y-axis reaches

12.12kN, the whole section of the intersection of the Circular Hollow Section and the sleeve produces plastic deformation. At this time, the stress nephogram of the connector can be shown in Figure 12.

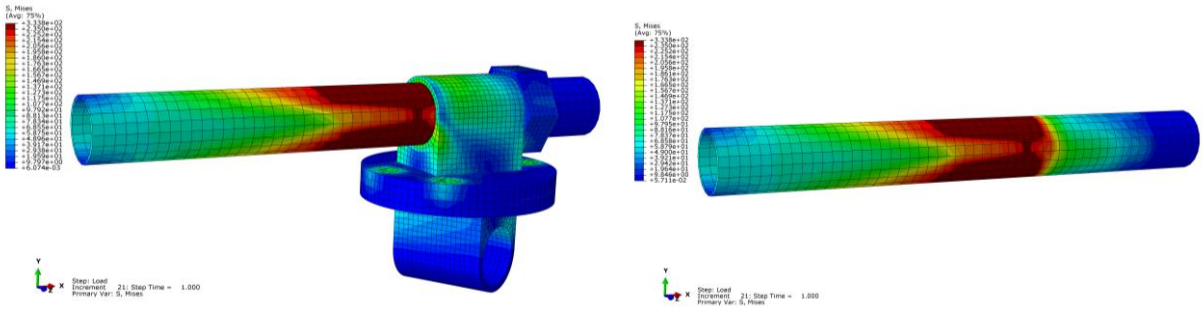

(a) Stress nephogram of the connector (b) The Circular Hollow Section

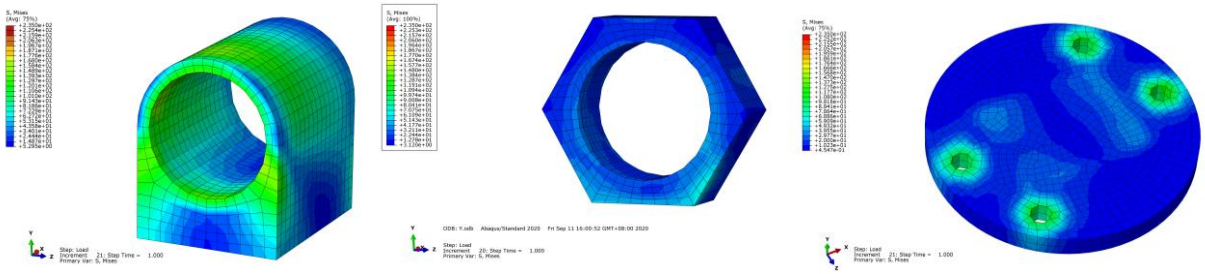

（c）The sleeve (d) The nut （e）The connecting plate

Fig. 12 - Stress nephogram of connector under Y-direction shearing force

It can be seen from Figure 12(b) that when the Y-direction shearing force reaches 12.12kN, the stress of the whole intersection of the Circular Hollow Section and the sleeve exceeds the material yield stress (235MPa), forming a plastic hinge. From Figure 12(c-e), the sleeve, nut and connecting plate are all in an elastic state. And the maximum stress of the sleeve is 175.7MPa, which is located on the inner wall of the sleeve near the external force. The maximum stress of the nut is 65.1MPa, which is located below the outer surface of the external force. The maximum stress of the connecting plate is 134.2MPa, which is located in the bolt hole far away from the external force. Take the rotation angle of the line around Z-axis connecting the sleeve's central point in front with its central point in the rear as the rotation angle of the connector around Z-axis. At this time, the rotation angle of this connector is only 8.3×10^{-4}rad, and the flexural rigidity of the connector around the Z-axis is very high. It can be seen that the structural damage is mainly caused by the plastic hinge formed at the end of the Circular Hollow Section when the members are subjected to the Y-direction shearing force. The adjustable connector of reciprocal frame has high strength and is still in an elastic state. The rigidity of the connector around the Z-axis is also great. When a plastic hinge is formed at the end of the Circular Hollow Section, the rotation angle of the connector around the Z-axis is minimal.

Under the condition of a shearing force parallel to the Z-axis being applied to the end section of the Circular Hollow Section, the applied shearing force is continuously increased until the plastic deformation of the whole Circular Hollow Section has formed in order to study the force characteristics and failure mechanism of the connector. Based on the analysis, the intersection of the Circular Hollow Section and the sleeve is still the maximum force section of the Circular Hollow Section. When the shearing force parallel to the Z-axis reaches 12.16kN, the whole section of the intersection of the Circular Hollow Section and the sleeve produces plastic deformation. At this time, the stress nephogram diagram of the connector is shown in Figure 13.

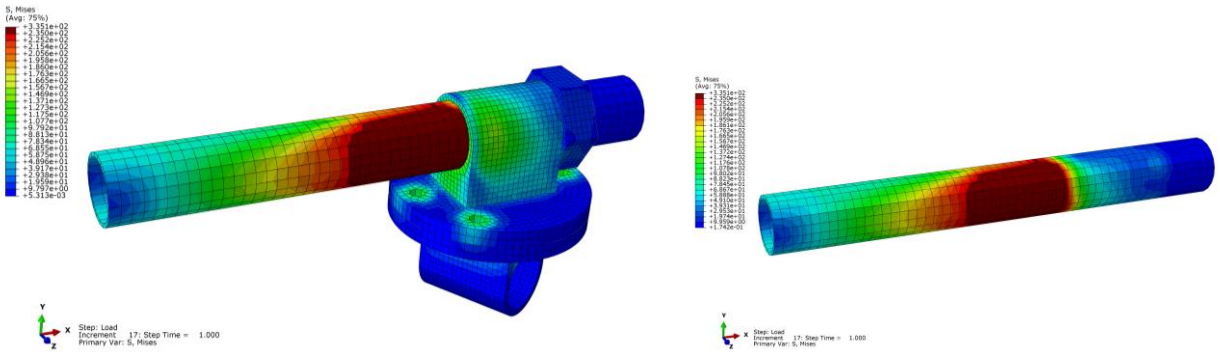

(a) Stress nephogram of the connector *（b）The Circular Hollow Section*

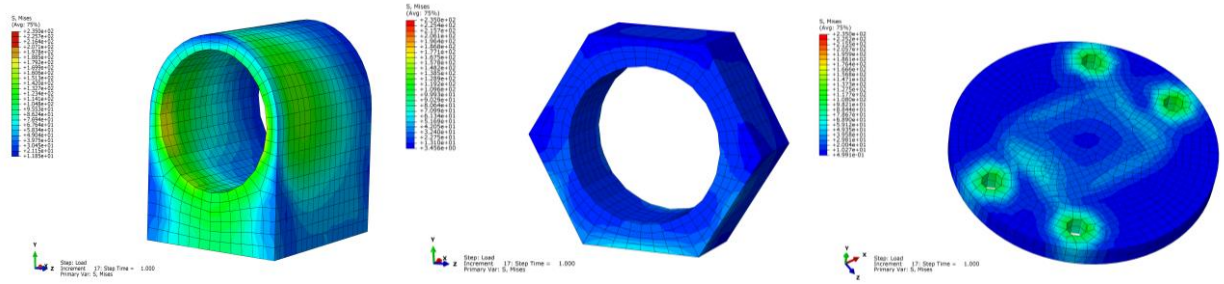

(b) The Circular Hollow Section (c) The sleeve (d) The nut (e)The connecting plate

Fig. 13 - Stress nephogram of connector under Z-direction shearing force

It can be seen from Figure 13(b) that when the Z-direction shearing force reaches 12.12kN, the stress of the whole intersection of the Circular Hollow Section and the sleeve exceeds the yield stress of the material by 235MPa, forming a plastic hinge. It can be seen from Figures 13 (c), 13 (d) and 13 (e) that the sleeve, nut and connecting plate are all in an elastic state. The maximum stress of the sleeve is 206.2MPa, which is located on the left side of the inner wall near the side where the external force is applied. The maximum stress of the nut is 63.1MPa, which is located at the bottom end of the surface near the side where the external force is applied. The maximum stress of the connecting plate is 127.7MPa, which is located in the bolt hole away from the external force. Take the rotation angle of the line around Y-axis connecting the sleeve's central point in front with its central point in the rear as the rotation angle of the connector around Y-axis. At this time, the rotation angle of the connector is only 1.01×10^{-3}rad, and the flexural rigidity of the connector around the Y-axis is very high. It can be seen that the structural damage is mainly caused by the plastic hinge formed at the end of the Circular Hollow Section when the members are subjected to Z-direction shearing force. The adjustable connector of reciprocal frame has high strength and is still in an elastic state. The rigidity of the adjustable connector of reciprocal frame around the Y-axis is also very large. When the end of the Circular Hollow Section forms a plastic hinge, the rotation angle of the connector around the Y-axis is minimal.

It can be concluded from the above-mentioned analysis that the strength of the adjustable connector of reciprocal frame is relatively high. When the reciprocal frames are subjected to the ultimate load, the damage is mainly caused by the plastic hinge formed at the end of the members, and the adjustable connector of reciprocal frame is still in an elastic state, which has realized the goal for designing higher connector strength over members strength. The rigidity of the adjustable connector of reciprocal frame is very large. When the plastic hinge is formed at the end of the Circular Hollow Section, the rotation angle of the connector is very small and can be ignored. Therefore, the rigid connector model can be used to simulate the adjustable connector of reciprocal frame.

Calculation model of the connector

The adjustable connector of reciprocal frame is composed of 4 parts, and the mechanical characteristics of the connector directly affect the entire mechanical response of the reciprocal frame. In order to calculate the response of reciprocal frame under various forces, the calculation model of adjustable connector should be established first. The parameterized calculation method is adopted to establish the calculation model of the connector. The reciprocal frame member mainly bears lateral load and thus the connector of reciprocal frame mainly bears the bending moment around the Z-axis. This section mainly discusses the calculation model of the connector around the Z-axis. The fastening bolts have tightened the upper and lower connecting plates according to the analysis, and the parameters in the connecting plates barely impact the bending resistance of the connector. The bottom of the sleeve is welded to the connecting plate, and the thickness l_3 of the lower wall of the sleeve has little effect on the flexural rigidity of the connector. The five parameters d_1、d_2、d_3、d_4 and l_3 in Figure 10 create minimal effect on the flexural rigidity of the connector around the Z-axis. The parameters d_1=360mm，d_2=16mm，d_3=20mm，d_4=25mm，and l_3=30mm, are fixed values. For the sake of parametric analysis, the values of l_1、l_2、l_4 and f are changed singly and 20 sets of numerical models are established. The 20 sets of model parameters are shown in Table 2.

Tab. 2 - Numerical model parameters

No.	1	2	3	4	5	6	7	8	9	10
l_1/*mm*	6	9	12	15	18	12	12	12	12	12
l_2/mm	120	120	120	120	120	60	90	120	150	180
l_4/*mm*	150	150	150	150	150	150	150	150	150	150
f	Q235	Q235	Q235	Q235	Q235	Q235	Q235	Q235	Q235	Q235
No.	11	12	13	14	15	16	17	18	19	20
l_1/*mm*	12	12	12	12	12	12	12	12	12	12
l_2/*mm*	120	120	120	120	120	120	120	120	120	120
l_4/*m*	90	120	150	180	210	150	150	150	150	150
f	Q235	Q235	Q235	Q235	Q235	Q235	Q255	Q275	Q295	Q345

A bending moment around the Z-axis is applied to the connector sleeve. Take the rotation angle of the line around Z-axis connecting the sleeve's central point in front with its central point in the rear as the rotation angle of the connector around Z-axis, and the bending moment of model 1~model 5 is calculated. As shown in Figure 14(a). The bending moment-rotation angle curve of model 6~model 10 is shown in Figure 14(b). The bending moment-rotation angle curve of model 11~model 15 is shown in Figure 14(c). The bending moment-rotation angle curve of model 16~model 20 is shown in Figure 14(d). From Figure 14 (a-d), it can be seen that the bending moment of the adjustable connector and the rotation angle is in a linear relation.

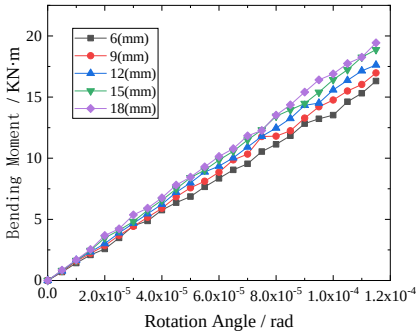

No. 1~5 Bending moment-rotation angle

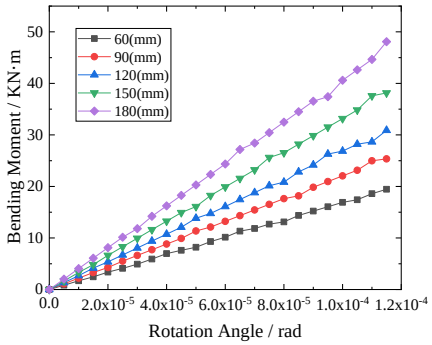

(b)No.6~10 Bending moment-rotation angle

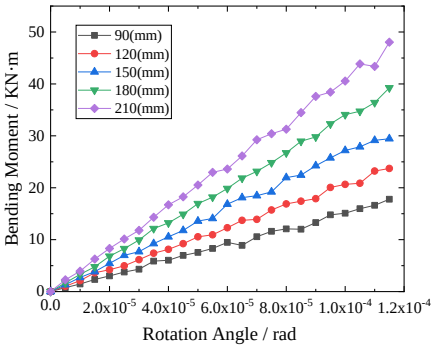

(c) No. 11~15 Bending moment-rotation angle

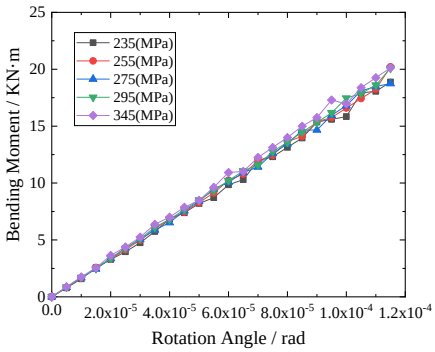

(d) No.16~20 Bending moment-rotation angle

Fig. 14 - Bending moment--rotation angle curve of the connector

According to Figure 14, the slope of each curve, that is the flexural rigidity of each connector model around the Z-axis, can be calculated by the least square method. In Model 1~Model 5, the effect of l_1 on the flexural rigidity of the connector around the Z-axis is achieved by changing the parameter of l_1. The flexural rigidity k of the connector around the Z-axis is shown in Table 3. The relation between l_1 and k is shown in Figure15.

Tab. 3 - Flexural rigidity of the connector model 1~5

No.	1	2	3	4	5
l_1/mm	6	9	12	15	18
k/(N·m/rad)	139226	147586	155864	164166	169000

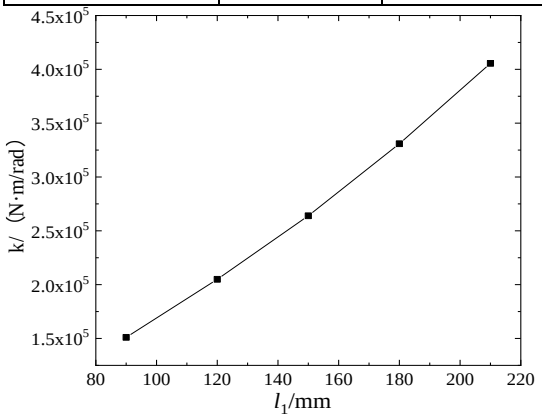

Fig. 15 - Relation curve between l_1 and k

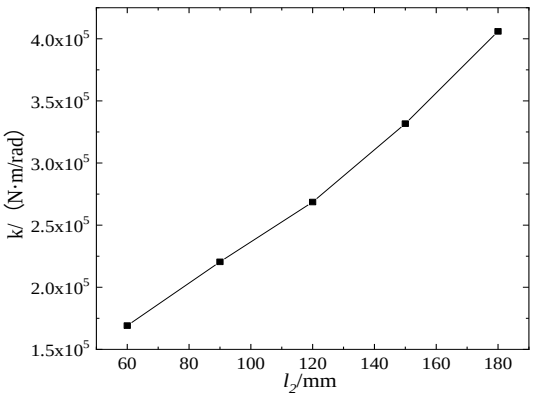

Fig. 16 - Relation curve between l_1 and k

Only the parameter l_2 has been changed in Model 6~Model 10. The flexural rigidity k of the connector around the Z-axis is shown in Table 4, and the relation curve between l_2 and k is shown in Figure 16.

Tab. 4 - Flexural rigidity of the connector model 6~10

No.	6	7	8	9	10
l_2/mm	60	90	120	150	180
k/(N·m/rad)	169116	220468	268590	331686	405976

Only the parameter l_4 has been changed in Model 11 ~ Model 15. The flexural rigidity l_4 of the connector around the Z-axis is shown in Table 5, and the relation curve between l_4 and k is shown in Figure 17.

Tab. 5 - Flexural rigidity of the connector model 11~15

No.	11	12	13	14	15
l_4/mm	90	120	150	180	210
k/(N·m/rad)	151036	204966	263960	330896	405544

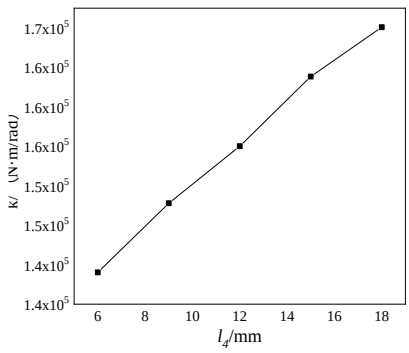

Fig. 17 - Relation curve between l4 and k

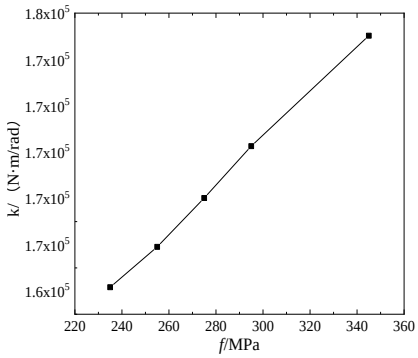

Fig.18 -Relation curve between f and k

In Model 16 ~ Model 20, only the parameter f has been changed. The flexural rigidity k of the connector around the Z-axis is shown in Table 6, and the curve of the relation between f and k is shown in Figure -18.

Tab. 6 - Flexural rigidity of the connector model 16~20

No.	16	17	18	19	20
f/MPa	235	255	275	295	345
k/(N·m/rad)	164166	165908	168018	170256	175026

It can be seen from Figure 15~Figure 18 that the flexural rigidity of the connector has a positive linear relation with the sleeve wall thickness l_1, the sleeve inner diameter l_2, the sleeve length l_4, and the material yield strength f. In order to study the quantitative relationship between the flexural rigidity of the connector and the related parameters, the same dimension parameters $k/\left(l_2 \cdot l_4 \cdot f\right)$ and l_1 are constructed. The relation between the two parameters is shown in Figure 19.

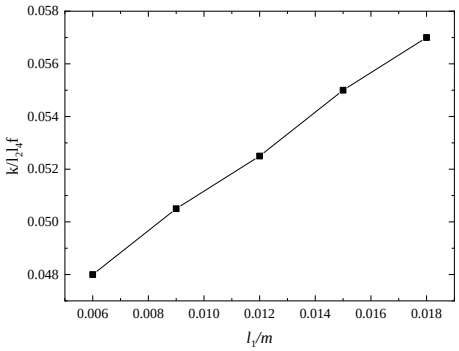

Fig. 19 - Relation curve between $k/\left(l_2 \cdot l_4 \cdot f\right)$ *and* l_1

$k/\left(l_2 \cdot l_4 \cdot f\right)$ and l_1 are in a linear relation from Figure 19, and the least square method is used for analysis to get a formula and correlation efficient as follows:

$$\frac{k}{l_2 \cdot l_4 \cdot f} = 0.75 l_1 \tag{1}$$

Correlation coefficient $R^2 = 0.9985$。

Therefore, the flexural rigidity of the adjustable connector of reciprocal frame is:

$$k = 0.75 l_1 l_2 l_4 f \tag{2}$$

NUMERICAL ANALYSIS OF RECIPROCAL FRAME

The members of the reciprocal frame mainly bear lateral loads. According to the analysis in section 3, the adjustable connector of reciprocal frame is of semi-rigid. Accurate numerical models should be established to research the mechanical characteristics of the connector. A three-dimensional wire model of reciprocal frame has been created in the FEM software Abaqus CAE. The members are simulated by beam elements, while the joints are simulated by UJoint connectors, and the UJoint connectors can be set rigidity value. Defining the UJoint connectors, according to the relation curve in Figure 19 and the formula (2) in Section 3.2, and the calculation model of reciprocal frame considering joint rigidity can be established. The support is hinged, that is, translational freedom of the support is constrained and rotational freedom is released. The members are Circular Hollow Section of Q235 with an outer diameter of 60mm, wall thickness of 3mm and length of 1500mm. The dimensions of each part in the adjustable connector of reciprocal frame are t_1=90mm, t_2=62mm, t_3=40mm, l_1=8mm, l_2=90mm, l_3=30mm, l_4=120mm, d_1=270mm, d_3=16mm, d_4=20mm. The angle between the member and the horizontal plane is 8°. A concentrated force of 540N, 840N and 1140N is applied at each joint in turn. A finite element model of reciprocal frame is shown in Figure 20.

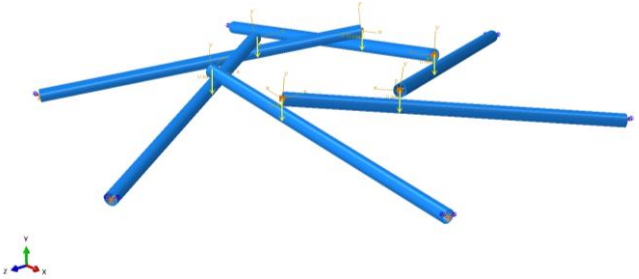

Fig. 20 - A finite element model of the reciprocal frame

After the static analysis, the deformation of the structure was amplified by 30 times to show the result of the members under the different concentrated force.

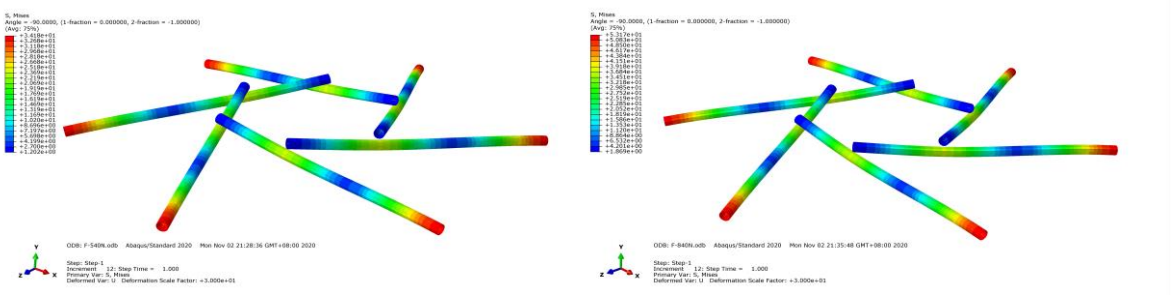

（a）Concentrated force of 540N *（b）Concentrated force of 840N*

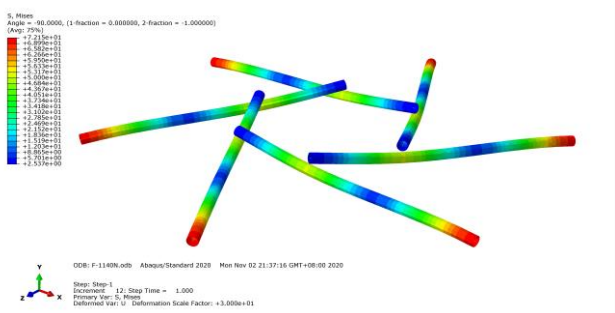

（c）Concentrated force of 1140N

Fig. 21 - Nephogram of structural stress under different concentrated forces

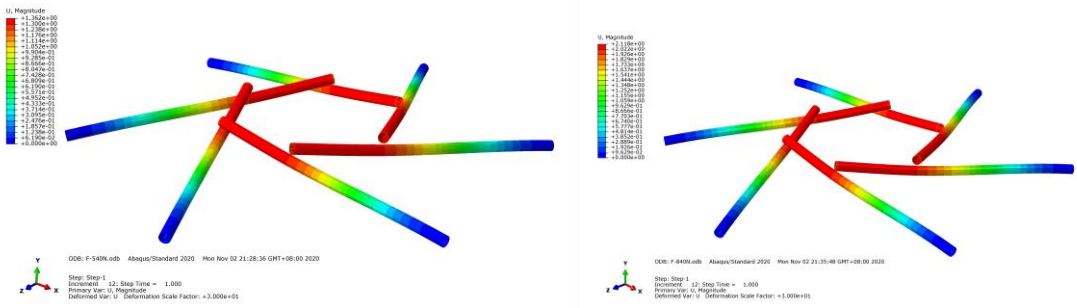

（a）Concentrated force of 540N *（b）Concentrated force of 840N*

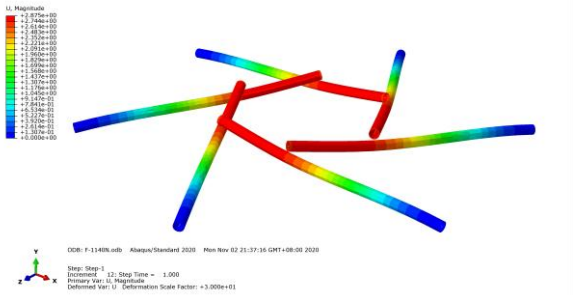

（c）Concentrated force of 1140N

Fig. 22 - Nephogram of structural vertical displacement under different concentrated forces

As seen in Figure 22, reciprocal frame is of rotational symmetry, which makes stress and deformation of each member uniform. The position of the maximum vertical displacement is at the joint and the position of the maximum stress is at the support. See Tables 6 and 7. The stress decreases first and then increases from the joint to the support of the member. The vertical displacement values of members between adjacent joint is uniform and larger than the rest.

Tab. 6 - Stress of the members under different concentrated force

Concentrated Force	540N	840N	1140N
maximum stress	34.2	53.2	72.1
stress at joint	24.1	37.4	50.8

Tab.7 - Vertical displacement of the joints under different concentrated force

Concentrated Force	540N	840N	1140N
Deformation	1.36	2.12	2.88

FULL-SCALE TEST

In order to verify the validity of the mechanical model and structural modeling method of the connector, carrying out a full-scale test including connectors and members. The full-scale test model is shown in Figure 21. The test model was fixed on a regular hexagon pedestal with great stiffness, and the end of members are welded to the pedestal. The size of members and connectors of the full-scale test model are the same as the numerical model in Section 4. The test model was loaded with weights.

The members are numbered A~F, and three measuring points are installed at the bottom of each member, which are respectively located at the joint of the member, the center of the joint and internal endpoint, and the center of the joint and external endpoint. There are 18 measuring points. For A~F members, measuring points are numbered successively from 1 to 18. According to electrical measures, the strain changes of each measurement point in the structure are measured through resistance strain gauge. According to the formula Hooke's law $\sigma = \mathrm{E} \cdot \varepsilon$, the stress of each measuring point can be calculated. Displacement meters are installed below the measuring points 2, 5, 8, 11, 14 and 17 in Figure 21 (a). The change of vertical displacement at the joints of members in the structure is measured.

（a） (b) (c)

Fig.21 - (a) Location of strain gage (b) Loading diagram (c) Displacement meter

As shown in Figure 21(b), a concentrated force of 540N, 840N and 1140N is applied at each joint respectively. The data of stress and vertical displacement at the joint points in members A~F are shown in Table 8 and Table 9.

Tab. 8 - Stress of the members under different concentrated forces/MPa

Member	Concentrated Force		
	540N	840N	1140N
A	36.6	56.2	76.3
B	34.2	49.6	79.4
C	36.5	57.5	69.6
D	35.7	51.2	78.9
E	35.5	55.3	64.
F	32.2	63.4	77.4
average	35.1	58.9	74.3

Tab. 9 - Vertical displacement of the joint under different concentrated forces/mm

Member	Concentrated Force		
	540N	840N	1140N
A	1.42	2.27	2.91
B	1.36	2.19	2.85
C	1.26	2.58	2.93
D	1.33	2.07	2.52
E	1.24	2.31	3.14
F	1.35	2.02	2.65
average	1.33	2.24	2.84

COMPARISON OF TEST RESULTS AND NUMERICAL SIMULATION RESULTS

Comparison of the results of stress between test and numerical simulation

Tab. 10 - Comparison under 540N concentrated force at the joints/MPa

member	A	B	C	D	E	F
test results	36.6	34.2	36.5	35.7	35.5	32.2
simulation results	34.2	34.2	34.2	34.2	34.2	34.2
relative error	6.5%	0	6.3%	4.2%	3.7%	6.2%

Tab. 11 - Comparison under 840N concentrated force at the joints/MPa

member	A	B	C	D	E	F
test results	56.2	49.6	57.5	51.2	55.3	63.4
simulation results	53.2	53.2	53.2	53.2	53.2	53.2
relative error	5.3%	7.3%	7.5%	3.9%	3.8%	16%

Tab. 12 - Comparison under 1140N concentrated force at the joints/MPa

member	A	B	C	D	E	F
test results	76.3	79.4	69.9	78.9	64.2	77.4
simulation results	72.1	72.1	72.1	72.1	72.1	72.1
relative error	5.5%	9.2%	3.1%	8.6%	12.3%	6.8%

It can be seen from the table that under different concentrated forces, the test results at the joints of each member are very close to the simulation results, and the error is very small.

Comparison of the results of vertical displacement between test and numerical simulation

Tab. 13 - Comparison under 540N concentrated force at the joints

member	A	B	C	D	E	F
test results /mm	1.42	1.36	1.26	1.33	1.24	1.35
simulation results /mm	1.36	1.36	1.36	1.36	1.36	1.36
relative error	4.2%	0	7.9%	2.3%	9.7%	0.7%

Tab. 14 - Comparison under 840N concentrated force at the joints

member	A	B	C	D	E	F
test results /mm	2.27	2.19	2.58	2.07	2.31	2.02
simulation results /mm	2.12	2.12	2.12	2.12	2.12	2.12
relative error	6.6%	3.2%	17.8%	2.4%	8.2%	4.9%

Tab. 15 - Comparison under 1140N concentrated force at the joints

member	A	B	C	D	E	F
test results /mm	2.91	2.85	2.93	2.52	3.14	2.65
simulation results /mm	2.88	2.88	2.88	2.88	2.88	2.88
relative error	1.0%	1.1%	0.7%	14.3%	8.3%	8.7%

It can be seen from the tables that under different concentrated forces, the test results at the joints of each member are very close to the simulation results, and the error is very little.

CONCLUSION

(1) In this paper, we design an adjustable connector of reciprocal frame which consists of a sleeve, a nut, two connecting plates and four bolts. A three-dimensional solid model of this connector with Circular Hollow Section has been created in the FEM software Abaqus CAE to study the mechanical properties of the connector. When the plastic hinge is formed at the end of the Circular Hollow Section, the connector is still in an elastic state. It is verified that the adjustable connector of reciprocal frame has high strength and rigidity, realizing the goal for designing higher connector strength over Circular Hollow Section strength.

(2) Under lateral load, parametric analysis is used to analysis the influence of the connector about each part on the mechanical properties. There is a linear relation between flexural rigidity and material yield strength, sleeve diameter, sleeve length, and wall thickness of the sleeve. Then the flexural rigidity of the connector is derived.

(3) A three-dimensional wire model of reciprocal frame has been created in the FEM software Abaqus CAE, and full-scale test model of the structure is designed. The numerical simulation results agree well with the test results. It is verified that the reliability of the modeling method and the accuracy of the mechanical model.

ACKNOWLEDGEMENTS

Financial supports from Fundamental Research Funds for Central Universities (3122019104) is gratefully acknowledged.

REFERENCES

[1] Fan Binghe, Luo Chao, Xu Xiaoyan, etc. Structural configuration analysis and detailing of wooden Rainbow Bridge[J].SPATIAL STRUCTURE,2018,24(01):91-96.doi: 10.13849/j. issn.1006-6578. 2018.01.091
[2] Yan Su, Makoto Ohsaki, Yue Wu, Jingyao Zhang. A numerical method for form finding and shape optimization of reciprocal structures[J]. Engineering Structures,2019,198
[3] Baverel, O., and H. Nooshin. 2007. Nexorades based on regular polyhedra. Nexus Network Journal 9(2): 281–299. doi: 10.1007/s00004-007-0043-0
[4] Bertin V. Leverworks : one principle, many forms [M]. Beijing: China Architecture & Building Press, 2012. 11-11.
[5] Larsen, Olga Popovic.Reciprocal Frame (RF) Structures: Real and Exploratory[J].Nexus network journal: Architecture and mathematics,2014,16(1):119-134. doi: 10.1007/s00004 -014-0181-0
[6] Bernard Vaudeville,Simon Aubry,Simon Gelez.Nexorade or Reciprocal Frame System Applied to the Design and Construction of a 850 m2 Archaeological Shelter [J]. International journal of space structures,2011,26(4):303-311. doi: 10.1260/0266-3511. 26.4.303
[7] Song, P.,-Wing Fu, C.,Goswami, P., et al.Reciprocal frame structures made easy[J].ACM Transactions on Graphics,2013,32(4 CD/ROM):94-1-94-10. doi: 10.1145/2461912.246 1915
[8] Alejandro Bernabeu Larena,David García Ménendez, et al.Extension of Euskalduna Conference Centre and Concert Hall: A Contemporary Application of Irregular Reciprocal Frames[J].Structural Engineering International,2014,24(1):63-67. doi: 10.2749/10168 66 14X13830788506233
[9] Yan Su,Makoto Ohsaki,Yue Wu,Jingyao Zhang. A numerical method for form finding and shape optimization of reciprocal structures[J]. Engineering Structures,2019,198. doi:10.1016/j.engstruct. 2019.109510
[10] Aicher, S., Garrecht, H., Reinhard, H.-W. (2014): Materials and Joints in Timber Structures. Springer, New York, pp. 129-134.
[11] Rizzuto J P, Popovic O L. Connection Systems in Reciprocal Frames and Mutually Supported Elements Space Structure Networks[J]. International Journal of Space Structures, 2010, 11(4): 243-256. doi: 10.1260/0266-3511.25.4.243
[12] Baverel, O., and H. Nooshin. 2007. Nexorades based on regular polyhedra. Nexus Network Journal 9(2): 281–299. doi: 10.1007/s00004-007-0043-0
[13] Bijnen A. Een geodetiese knoopkonstruktie[P]. Octrooiraad Nederland, Terinzagelegging. Aanvrage, No 7603046. 1976.
[14] JOEL GUSTAFSSON. Connections in Timber Reciprocal Frames[D]. Gothenburg, Sweden: CHALMERS UNIVERSITY OF TECHNOLOGY,2016.
[15] Liu Xuechuan,Shang Zixuan, Zhang Dongjie,etc.Research key points and present situation analysis of prefabricated multi-story and high-rise steel structures[J].Industrial Construction, 2018, 48(05):1-10. doi: 10.13204/j.gyjz201805001
[16] O. Baverel,O . Popovic Larsen. A Review of Woven Structures with Focus on Reciprocal Systems Nexorades[J]. International journal of space structures,2011,26(4):281-288. doi:10.1260/0266-351 1.26.4.281
[17] Rizzuto J P. The Structural Behaviour of Mutually Supported Elements in Space Structures[D]. Coventry: Coventry University, 2005.
[18] J. P. RIZZUTO. Rotated Mutually Supported Elements In Truncated Icosahedric Domes [J] Journal of the international association for shell and spatial structures, 2007, 48(1):3-17.
[19] Maziar Asefi, Mahnaz BahremandiTolou. Design challenges of reciprocal frame structures in architecture[J]. Journal of Building Engineering,2019,26.
[20] Larsen, Olga. (2014). Reciprocal Frame (RF) Str Exploratory. Nexus Network Journal. 16. 10.1007/s00004-014-0181-0. doi: 10.1007/s00004-014-0181-0